Available online at www.sciencedirect.com

ScienceDirect

RESEARCH PAPER

Liquid Phase Hydrogenation of Benzalacetophenone: Effect of Solvent, Catalyst Support, Catalytic Metal and Reaction Conditions

Achim STOLLE[1],*，Christine SCHMÖGER[1], Bernd ONDRUSCHKA[1], Werner BONRATH[2], Thomas F. KELLER[3], Klaus D. JANDT[3]

[1]Institute for Technical Chemistry and Environmental Chemistry (ITUC), Friedrich-Schiller University Jena, Lessingstrasse 12, D-07743 Jena, Germany

[2]R&D Chemical Process Technology, DSM Nutritional Products, P.O. Box 2676, CH-4002 Basel, Switzerland

[3]Institute of Materials Science and Technology (IMT), Friedrich-Schiller University Jena, Löbdergraben 32, D-07743 Jena, Germany

Abstract: Innovative catalysts based on a "porous glass" support material were developed and investigated for the reduction of benzalacetophenone. The easy preparation conditions and possibility to use different metals (e.g. Pd, Pt, Rh) for impregnation gave a broad variety of these catalysts. Hydrogenation experiments with these supported catalysts were carried out under different hydrogen pressures and temperatures. Porous glass catalysts with Pd as the active component gave chemoselective hydrogenation of benzalacetophenone, while Pt- and Rh-catalysts tended to further reduce the carbonyl group, especially at elevated hydrogen pressures and temperatures. Kinetic analysis of the reactions revealed these had zero order kinetics, which was independent of the type of porous glass support and solvent used.

Key words: chalcone; hydrogenation; porous glass; supported catalyst

The reduction of unsaturated bonds is important in the syntheses of fine chemicals such as vitamins, flavours, and fragrances [1,2]. The chemical industry often employs gaseous hydrogen as the reducing reagent due to its excellent atom efficiency. Hydrogenation is used in the processing of vegetable oils and fats and in the crude oil and coal industries [3–5]. In contrast, on the laboratory scale, catalytic transfer hydrogenation (CTH) is often the method of choice [6] due to less hazardous handling and convenient laboratory equipment. Formic acid (or its salts), hydrazine, or cyclohexene derivatives are common reducing reagents, and are most often used in connection with a heterogeneous or homogeneous catalyst (e.g. Ni-alloy, Ru-complexes) [7,8]. The use of gaseous hydrogen and a heterogeneous catalyst in the liquid phase would combine their advantages. The easy recovery of catalyst, good yield and selectivity, and a high atom efficiency of the hydrogenation with H_2 are some of the advantages.

The use of gaseous hydrogen for reduction reactions in connection with microwave irradiation is unusual and only a few papers on it have been published to date [6,9,10]. Part of the following work used reduction with gaseous hydrogen in a microwave apparatus. A new reactor named QRS (quartz-reactor-system) was developed to carry out hydrogenation under moderate pressures (≤ 0.8 MPa) and temperatures (≤ 200 °C) on the laboratory scale. Commercially available steel autoclaves were used for liquid phase hydrogenation under higher pressures (≤ 5.0 MPa).

The model substrate used for the liquid phase hydrogenation was 1,3-diphenylprop-2-en-1-one (**1**; Scheme 1), often called benzalacetophenone or chalcone. Chalcones are essential in the pharmaceutical industry because of their antibiotic or bacteriostatic properties [11]. They are part of a family of aromatic ketones with two aromatic groups bridged by an enone linkage. Usually they are prepared by base- or acid-catalyzed aldol condensation of aromatic aldehydes and the respective acetophenones [11,12]. The solvent-free preparation with the use of
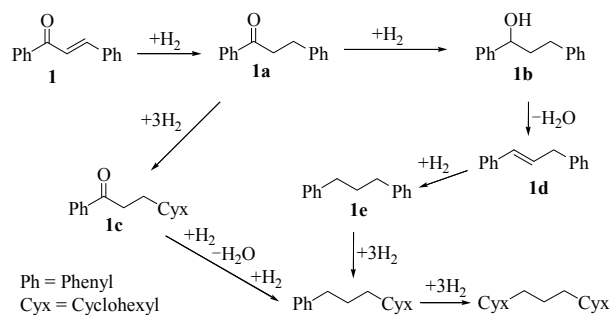
Scheme 1. Reaction scheme for the reduction of benzalacetophenone (**1**) with H_2 and supported metal catalysts.

acidic clays is also possible [13]. Stoichiometric amounts of benzaldehyde and acetophenone are the raw materials for the preparation of **1**. The reduction of the C-C double bond in **1** leads to the saturated ketone 1,3-diphenylpropan-1-one (**1a**), which is an intermediate for the Friedländer quinoline synthesis [14]. It is also an interesting building block for enol carbonates [15].

The aim of this study was to determine the influence of various reaction parameters in the liquid phase hydrogenation of benzalacetophenone catalyzed by metal-loaded porous glasses. Various catalytically active metals and support materials used at different reaction temperatures and hydrogen pressures were tested. To cover the required temperature and pressure range, three different apparatuses were used.

1 Experimental

1.1 Preparation of the catalysts

Table 1 summarizes the important parameters (e.g. surface area, pore size) of the support materials for the preparation of the catalysts. The metal precursors and corresponding solvents employed are listed in Table 2. The porous glass supports (Table 1, entry 1–8) were purchased from VitraBio (Stein-

ach/Germany). The remaining support materials, substrates, metal precursors, and solvents were from Sigma-Aldrich. The chemicals were used without further purification. The purities of the solvents and starting materials were checked by gas chromatography (GC) prior to use.

In a round bottom flask (100 ml), the metal component (0.09 mmol) was dissolved in an adequate amount of solvent (50 ml; Table 2). The support material (1 g; Table 1) was added to the mixture. After equilibration (stirring, 30 min), the solvent was removed in vacuo. Subsequently, the catalyst precursor was calcined for 2 h at 300–450 °C (corresponding to the decomposition temperature of the metal compound, Table 2) in a muffle furnace "mls 1200 pyro" (MLS GmbH, Leutkirch, Germany) resulting in a catalyst with a metal loading of 0.09 mmol/g. Calcination temperatures above 450 °C cannot be realized, because the porous texture of the porous glasses. BET-analyses showed that higher temperatures lead to a significant decrease of specific surface area. In contrast, longer reaction times (4 or 6 h) show no influence on the porosity of the porous glass support.

The preparation of catalysts with two metal components used a modification of the procedure described above. The catalyst Ce/Pd/TP(I) was prepared by one impregnation step. Here, both metal components (each with 0.09 mmol) were dissolved in 50 ml solvent. After removal of the solvent, the catalyst precursors were also calcined at the corresponding temperature. The catalyst Ce/Pd/TP(II) was prepared by double impregnation. After impregnation with one metal component (0.09 mmol) and calcination, a second impregnation step followed with the other metal component (also 0.09 mmol). The impregnations were performed in the same way as described above.

1.2 Characterization of the catalysts

TGA analyses of the metal precursors were carried out with a Shimadzu DTG-60 simultaneous DTA-TG apparatus

Table 1 Selected parameters of the support materials

Entry	Support name	Notation	d_{50}/µm	d_p/nm	S_V/(m²/g)	V_p/(mm³/g)
1	TRISOPOR®	TA	50–90	51	89	1215
2	TRISOPOR®	TB	100–200	50	98	1321
3	TRISOPOR®	TC	315–500	49	75	1115
4	TRISOPERL®	TPA	50-100	55	96	1213
5	TRISOPERL®	TP	100–200	55	94	1256
6	TRISOPOR®	A	1250	45	85	759
7	TRISOPOR®	B	800–2500	173	20	711
8	TRISOPOR®	C	800–2500	300	14	664
9	silica	SiA	35–45	17–23	110–180	600–1000
10	silica	SiB	35–45	26–34	70–170	600–1000
11	silica	Si1	105–200	—	500–600	—
12	alumina	Al1	110	—	50	—

d_{50} = average particle diameter, d_p = average pore size, S_V = average specific surface area, V_p = average specific pore volume; d_p, S_V, and V_p were calculated from data of 6-point BET measurements and are in agreement with the data provided by the manufactures.

Table 2　Metal precursors, the required solvents, and calcination temperatures for the preparation of the various catalysts

Catalyst	Metal precursor	mp_{Lit}[a]/°C	Solvent[b]	T[c]/°C
Pd/Support[d]	Pd(AcO)$_2$	205 (dec.)	dichloromethane	300
Pd-A/TP	PdCl$_2$	675 (dec.)	HCl$_{aq}$ (5%)	450
Ce/Pd/TP(I)	Ce(acac)$_3$ + Pd(AcO)$_2$	131/205	dichloromethane	300
Ce/Pd/TP(II)	Ce(acac)$_3$/Pd(AcO)$_2$	131/205	dichloromethane	300
Pt/TP	Pt(acac)$_2$	249–252	acetone	300
Rh/TP	RhCl$_3$·H$_2$O	100	acetone	450
Rh-A/TP	Rh(acac)$_3$	263–264	acetone	300
Ru/TP	RuCl$_3$·H$_2$O	>500 (dec.)	acetone	450
Ru-A/TP	Ru(acac)$_3$	260 (dec.)	acetone	300
Ir/TP	Ir(acac)$_3$	269–271	acetone	300
Co/TP	Co(acac)$_3$	211 (dec.)	acetone	300
Ni/TP	Ni(NO$_3$)$_2$·6H$_2$O	56	acetone	450
Ag/TP	Ag(hfacac)(COD)	122–124	acetone	300
Au/TP	HAuCl$_4$·3H$_2$O	254 (dec.)	acetone	300
Fe/TP	Fe(acac)$_3$	180	acetone	300

[a]Melting point of metal precursor according to literature (confirmed by TGA). [b]Solvent used for catalyst preparation. [c]Calcination temperature (calcination time: 2 h inclusive preheating time 20 min). [d]All supports from Table 1. dec. – Decomposition.

(T-ramp: 10 °C/min). Transmission electron microscopy (TEM) micrographs were recorded with a transmission electron microscope H7500 from Hitachi (120 kV, LAB6 filament). The scanning electron microscopy (SEM) images were measured using a scanning electron microscope DSM 940 (Carl Zeiss). Optical microscopy pictures were recorded with a Stemi 2000-C microscope (Carl Zeiss; magnification: (6.5–50)×; cold light source KL 1500 LCD) in combination with a digital camera JVC GZ-MC200E (2 mega pixel; 10× optical zoom). 6-Point BET measurements were carried out with an Autosorb1 (Quantachrome) using N$_2$ as sorbent gas and a heating temperature of 350 °C. X-ray photoelectron spectroscopy (XPS) spectra were recorded with a Quantum 2000 (PHI Co.) employing a focused monochromatic Al K_α source (1486.7 eV) for excitation. The pass energy was set to 23.5 eV and as reference, the C 1s peak of the C–C bond was used.

1.3　Reduction reactions

Three different experimental setups were required for the reduction reactions because different temperatures and pressures were used. The following equipments were used. Setup A: room temperature (25 °C) and atmospheric pressure. Setup B: pressure ≤ 0.8 MPa, temperature ≤ 50 °C. Setup C: pressure ≤ 5.0 MPa, room temperature (25 °C).

1.3.1　Reactions in setup A

Benzalacetophenone (**1**, 15 mmol, 3.12 g) and 200 μl hexadecane (internal standard) were dissolved (60 ml solvent) and put into a Schlenk flask. After adding the catalyst (400 mg, 0.24 mol%), a sample was taken (500 μl). The Schlenk flask was connected to the hydrogen reservoir by a plug valve. The reaction vessel was flushed with hydrogen (400 ml × 3). The liquid phase hydrogenation reactions were carried out at atmospheric pressure and room temperature in a shaking apparatus "HS 501 digital" (IKA Labortechnik, Staufen, Germany). Every 20 min (after 60 min reaction time every 30 min), a sample (500 μl) was taken. The hydrogenation process was observed by the consumption of hydrogen and by analyzing the samples with GC-FID and GC-MSD.

1.3.2　Reactions in setup B

Benzalacetophenone (**1**, 7.5 mmol, 1.56 g), 100 μl hexadecane (internal standard), catalyst (200 mg, 0.24 mol%), and ethyl acetate (30 ml) were put into a quartz reactor vessel. The vessel was placed in a microwave equipment (multisynth, MLS GmbH, Leutkirch, Germany) and connected to the hydrogen reservoir. The use of a gas inlet allowed the direct flushing of hydrogen into the reaction mixture. The gas was continuously let off with a gas outlet valve to get a uniform gas flow (0.2 ml/min) through the reaction mixture. The liquid phase hydrogenation reactions were carried out at various pressures (0.2–0.8 MPa), temperatures (20–50 °C), and reaction times (0–40 min). The reaction temperature was measured and controlled using an ACT-CE sensor placed directly in the reaction solution. The reaction temperature of 25 °C was maintained by cooling the reactor with pressurized air. The hydrogenation process was observed by analyzing the samples with GC-FID and GC-MSD.

1.3.3　Reactions in setup C

Reduction at higher pressures were carried out in a commercial steel autoclave (Berghoff, Germany) equipped with a 100 ml PTFE insert. The reaction was controlled with pressure and temperature sensors equipped with the sealed autoclave.

Benzalacetophenone (**1**, 7.5 mmol, 1.56 g), 100 μl hexadecane (internal standard), catalyst (200 mg, 0.24 mol%), and ethyl acetate (30 ml) were put into a Teflon vessel inside the steel autoclave. The reaction vessel was flushed with nitrogen (1.0 MPa × 3). Afterwards the desired hydrogen pressure was set up. The liquid phase reduction reactions were carried out at different pressures (1.0–5.0 MPa) and reaction times (30–60 min). The hydrogenation process was observed by analyzing the samples with GC-FID and GC-MSD.

1.3.4 Analysis of the reduction reaction

The analyses of the reaction mixtures were carried out with GC-FID (Agilent 6890) and GC-MSD (Agilent 6890 N/5973 MS).

Conditions of GC-FID. Column: HP 5, 30 m × 0.32 mm × 0.25 μm; Carrier gas: H_2, 68.9 kPa; program: 60 °C (hold 1 min), 25 °C/min up to 280 °C (hold for 12 min); injector temperature: 280 °C; detector temperature: 300 °C.

Conditions of GC-MSD. Column: HP 5, 30 m × 0.32 mm × 0.25 μm; Carrier gas: He, 68.9 kPa; program: 60 °C (hold 1 min), 25 °C/min up to 280 °C (hold for 12 min); injector temperature: 280 °C; EI: 70 eV.

Conversion, yield, and selectivity were calculated based on corrected peak areas using hexadecane as the internal standard. All results were averages of at least two experiments.

2 Results and discussion

2.1 Catalyst characterization

Porous glasses have been applied as the support material for Pd catalysts in the hydrogenation of alkenes and alkynes [17–19], Suzuki-Miyaura [20], and Mizoroki-Heck cross-coupling [20,21] and for the partial hydrogenation of citral to citronellal [19]. The catalysts on the porous glasses or support materials with similar properties were characterized with different methods. The support materials TRISOPOR® (Table 1, entries 1–3 and 6–8) and TRISOPERL® (Table 1, entries 4 and 5) were the focus of these investigations. In particular, the two types of nano-structured glasses, TB and TP, were examined because most of the following liquid phase hydrogenation was carried out with catalysts on these supports. The two materials differ only in their external form but not in the parameters of d_{50} and S_V (Table 1, entries 2 and 5). Both support materials are commercially available and have been prepared by the same method (alkaline leaching of phase-separated borosilicate glasses) [22–27].

First, the particles were examined with optical microscopy. The optical resolution of this method allowed the retrieval of information on the geometric texture of the particles, but it was not enough to see the pore structure of the isolated particles ($d_p \leq 60$ nm). Figure 1 shows the photos of the two porous support
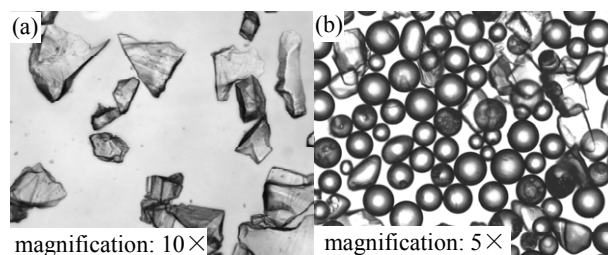

magnification: 10×   magnification: 5×

Fig. 1. Optical microscopy images of porous glasses TB (a) and TP (b).

materials prior to impregnation with the metal precursor. TB consisted of irregular aspheric particles with sharp broken edges, while the TP particles were regular and spherical. Regarding the particle shapes of TB and TP, the outer particle surface areas were higher for the aspheric particles than for the ball-shaped particles. Due to the porous structure of these materials, the influence of the outer surface on S_V was rather small due to the high pore volume (V_p; Table 1). The dispersion of the particles sizes was $100 \leq d_{50} \leq 200$ μm.

The detailed structure of the catalysts (porous glass impregnated with metal) was determined by SEM (Fig. 2) and TEM (Fig. 3). Catalysts Pd/TB and Pd/TP were chosen for measurement. The photos revealed the open porous structure and the SiO_2 network of the catalyst. The Pd clusters (5 nm ≤ cluster size ≤ 50 nm) were clearly seen on the surface (bright points in the SEM and dark points in the TEM micrographs). The measurements revealed that there was no complete coverage of the surface. The dispersion of the Pd particles on the surface could not be found because of the irregular spherical structure of the support material and its nano-porous structure. The micrographs indicated a narrow pore size distribution and no hierarchical porosity.

XPS was used to identify the oxidation state of the metals and to deduce the catalytically active form of the catalysts. XPS data of selected catalysts that showed good catalytic activity (cf. following sections) are listed in Table 3. The difference in binding energies (E_B) between the oxidation states of
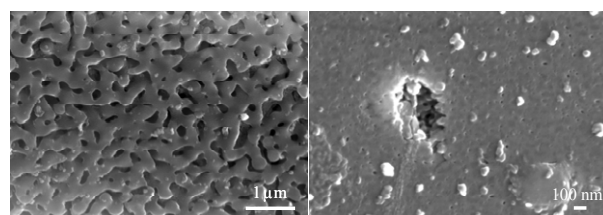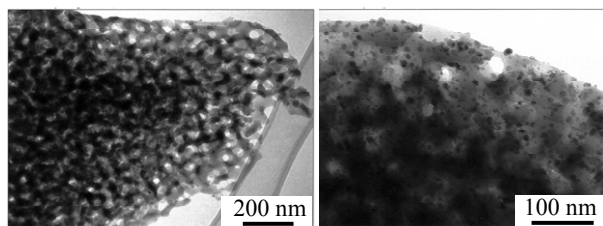

Fig. 2. SEM micrographs of Pd/TP.

Fig. 3. TEM micrographs of Pd/TB.

Table 3 XPS data of selected catalyst prepared by wet impregnation of the support material TP

Catalyst[a]	Core level	Binding energy of catalysts (eV)		
		Before calcination[b]	After calcination[c]	After application[d]
Pd/TP	Pd $3d_{5/2}$	336.8	336.1	335.3
	Pd $3d_{3/2}$	341.7	341.3	340.3
Pd-A/TP	Pd $3d_{5/2}$	336.5	336.2	335.9
	Pd $3d_{3/2}$	341.8	341.5	341.2
Ce/Pd/TP(I)	Pd $3d_{5/2}$	336.4	336.0	335.5
	Pd $3d_{3/2}$	341.8	341.4	340.5
	Ce $3d_{5/2}$	885.7	885.8	885.7
	Ce $3d_{3/2}$	905.8	905.8	905.7
Ce/Pd/TP(II)	Pd $3d_{5/2}$	336.4	336.0	335.5
	Pd $3d_{3/2}$	341.9	341.2	340.8
	Ce $3d_{5/2}$	885.7	885.8	885.7
	Ce $3d_{3/2}$	905.8	905.6	905.6
Pt/TP	Pt $4f_{7/2}$	71.8	71.8	72.8
	Pt $4f_{5/2}$	75.2	75.2	76.0
Rh/TP	Rh $3d_{5/2}$	308.4	308.3	308.2
	Rh $3d_{3/2}$	312.7	312.8	312.8
Rh-A/TP	Rh $3d_{5/2}$	308.7	309.3	307.6
	Rh $3d_{3/2}$	313.4	313.4	312.2

[a]Metal loading 0.09 mmol/g. [b]Impregnation with metal precursors listed in Table 2. [c]Calcination for 2 h in air atmosphere (for temperature see Table 2). [d]Hydrogenation of **1** at room temperature and atmospheric pressure (15 mmol **1**, 0.24 mol% metal/TP, 60 ml ethyl acetate).

the metal was rather small ($\Delta E \approx 2$–3 eV). For this reason, the catalysts were analyzed before and after calcination (time and temperature data given in Table 2) as well as after their use in the hydrogenation of **1** (Scheme 1). This procedure ensured comparable measurement conditions with respect to the metal-coordination sphere and surface concentration of the metal. Thus the results obtained can be compared and interpreted with a better accuracy by comparison with bulk metal compounds of different oxidation states. The XPS data shown in Table 3 did not indicate any metal-support interaction. All values were typical for metals supported on oxide materials like alumina and silica. Distinguishing between the metal layers in contact with the support material and those on the surface of the metal particle was not possible. Therefore, no effect of the support on the oxidation state was found.

The interpretation of the Pd/TP XPS data set is clearly described in the literatures [14–27]. The corresponding Ce containing catalysts (Ce/Pd/TP(I) and Ce/Pd/TP(II)) showed, in case of Pd, the same shift of E_B as Pd/TP. The difference between the two catalysts was in their preparation method. In the case of Ce/Pd/TP(I), both metals were co-impregnated from one solution, while in the other case, Pd was deposited before wet impregnation with Ce(acac)$_3$. Thus, an additional calcination step was used to anchor the Pd before the decoration with Ce. A comparison of the Ce binding energies showed no significant change in E_B for the two standard Ce peaks (Ce $3d_{5/2}$ and Ce $3d_{3/2}$) [28,29]. The constant E_B indicated no incorporation of the Ce component during the use of these catalysts. Furthermore, the broad peaks obtained showed that two oxidation states of Ce (+3 and +4) existed on the surface, which

was probably due to incorporation into the SiO$_2$ network of the glass carrier. A bonding to Pd did not occur since the shift for the Pd $3d$ was similar to that observed for Pd/TP (Table 3).

In case of Pt/TP, two characteristic peaks at 71.8 (Pt $4f_{7/2}$) and 75.2 eV (Pt $4f_{5/2}$) were present (Table 3) [30,31]. A shift to higher E_B was detected after the catalyst was used in the reduction reaction, which showed a partial change in oxidation state had taken place. This oxidation state was not studied in detail because all the possible Pt oxidation states (+2, +4) were active in the hydrogenation reaction.

The Rh-containing catalysts, Rh/TP and Rh-A/TP, differed only in the metal precursor used, which were RhCl$_3$·H$_2$O and Rh(acac)$_3$, respectively. The characteristic E_B for the Rh signals were at 308 and 313 eV for the Rh $3d_{5/2}$ and $3d_{3/2}$ core levels, respectively (Table 3) [32]. The E_B of both peaks and catalysts showed no significant change before and after calcination. That is, the oxidation state was not changed by calcination in air. The use of Rh-A/TP in a hydrogen atmosphere gave a shift to smaller E_B, which indicated the oxidation state change from +3 to Rh(0) for the spent catalyst. The catalyst Rh/TP did not show this shift after it was used. This difference was attributed to the precursor compound RhCl$_3$ used, which left residual Cl on the surface and inhibited the reduction from +3 to Rh(0).

2.2 Liquid phase hydrogenation at room temperature and atmospheric pressure

The liquid phase hydrogenation of **1** was chosen as the model reaction (Scheme 1). The molecule structure has different unsaturated groups: i) a conjugated C-C double bond, ii)

a carbonyl group, and iii) aromatic C-C double bonds. The degree of reduction and reaction rate of the hydrogenations depended on several parameters like the type of metal and support material, hydrogen pressure, and reaction temperature. First, the influence of support material in the liquid phase hydrogenation of **1** at room temperature and atmospheric pressure was studied (Table 4). In this case, the reduction experiments were carried out with palladium as the active metal. Thus, a comparison of the selected support materials in the reduction of **1** was possible. The various support materials are listed in Table 1. Mainly, porous glasses were used (Table 1, entries 1–8). They belong to the group of leached phase separated borosilicate glasses (SiO_2 content ≥ 96 %; confirmed with EDX) and offer the advantages as the support of chemical inertness, flexible texture, and narrow pore size distribution [17–23]. In addition, three different silica gels (Table 1, entries 9–11) and one alumina (Table 1, entry 12) were used to compare conventional support materials with the relatively unknown porous glass systems of TB and TP. When 0.24 mol% Pd (catalyst loading 0.09 mmol/g) was used, all the experiments gave the same reduction product 1,3-diphenylpropan-1-one (**1a**, Scheme 1). In all cases, the hydrogenation was chemoselective under the selected reaction conditions since only the conjugated C-C double bond was reduced. Furthermore, the support material had no influence on the selectivity but only on the reaction rate of the hydrogenation.

The rate constants k_1 and k_2 were calculated from the time dependent hydrogen uptake curves for the hydrogenation reaction. The use of a pseudo-zero order of reaction gave k_1, which indicated that the reaction was diffusion controlled and the reaction gas hydrogen was the limiting reactant at the beginning of the process. The reaction became substrate controlled (k_2) with the decrease of substrate concentration, thus the reaction order changed to pseudo-first order kinetics. The comparison of k_1 for the different catalysts revealed compara-

ble rates for the porous glass supports and conventional support materials. The activities were nearly the same for the porous glass systems (Table 4, entries 1–5) and silica-based catalysts (Table 4, entries 9–11). The lowest rate constants and conversions were found with the porous glass catalysts Pd/A, Pd/B, and Pd/C. It was probable that increasing the particle sizes in conjunction with decreasing S_V decreased mass transport and metal dispersion on the catalyst surface (Table 1) resulted in decreased reaction rates. Particularly good results were obtained with the systems Pd/TB and Pd/TP. A conversion of 75% was obtained after 120 and 150 min, respectively. The difference between the TB and TP supports was the geometrical shape of the particles (Fig. 1). The difference in particle morphology had no direct influence on the hydrogenation as shown by the similar initial reaction rates (Table 4) and kinetic profiles (Fig. 4). Thus, the similarity with respect to the physical properties (d_{50}, d_p, S_V and V_p; cf. Table 1) showed they were equal when applied as the support material in catalysis. The
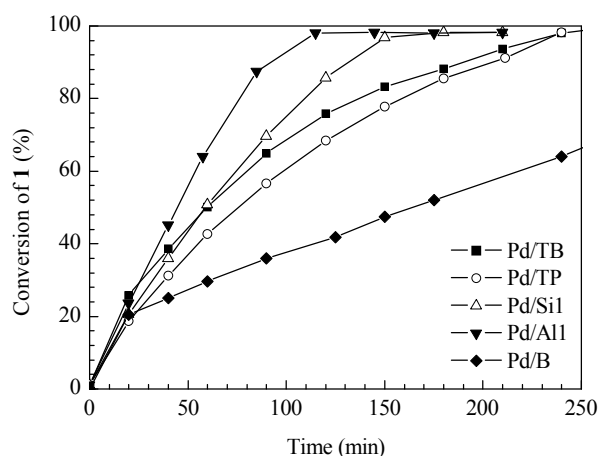

Fig. 4. Conversion of **1** by selected supported Pd catalysts at room temperature and atmospheric pressure. Reaction conditions are the same as in Table 4.

Table 4 Rate constants (k_1 and k_2) and time for 25%, 50%, and 75% conversion of **1** using various supported Pd-catalysts

Entry	Catalyst[a]	k_1[b]/(ml$_{H2}$/min)	k_2[b]/min^{-1}	Time for conversion of **1** (min)		
				25%	50%	75%
1	Pd/TA	2.705	0.0025	30	85	145
2	Pd/TB	3.014	0.0020	20	60	120
3	Pd/TC	2.751	0.0018	20	60	100
4	Pd/TPA	2.779	0.0024	30	70	140
5	Pd/TP	2.844	0.0026	30	75	150
6	Pd/A	0.930	0.0008	80	240	420
7	Pd/B	1.240	0.0009	40	175	300
8	Pd/C	0.940	0.0030	75	220	375
9	Pd/Si1	2.802	0.0008	25	60	100
10	Pd/SiA	2.738	0.0025	30	70	120
11	Pd/SiB	1.944	0.0032	40	90	145
12	Pd/Al1	3.672	0.0011	20	45	80

Reaction conditions: substrate **1** 15 mmol, catalyst 0.4 g (0.24 mol% Pd), ethyl acetate 60 ml, $T = 25$ °C, $p(H_2)$ = ambient pressure. [a]Pd loading 0.09 mmol/g. [b]The rate constants k_1 and k_2 were estimated with linear regression. Following acceptances are made: liquid-phase hydrogenation is a reaction of pseudo zero-order and become a reaction of pseudo first-order at the end of reaction time.

time versus conversion curves of **1** for selected catalysts are shown in Fig. 4. The curves showed complete conversion of **1** after 210 min for all the catalysts except Pd/B. In summary, the results demonstrated that the porous glasses can be used as support material in heterogeneous catalysis, especially in liquid phase hydrogenation [17–19]. The porous glasses TB and TP were used as the standard support for the catalysts and used in the following reactions.

Further experiments used the variation of different parameters during the liquid phase hydrogenation under room temperature and atmospheric pressure. First, the metal loading of the catalyst system Pd/TB was varied in the range of 0.1–2 wt% Pd. The curves of time versus conversion of **1** with 0.4 g of catalyst are shown in Fig. 5(a). The catalysts with a Pd loading of 1 wt% and higher gave complete conversion within 210 min. A decrease of the Pd amount on the support led to a decrease in the conversion of **1** to **1a** since less active metal centers were available. For this reason, all subsequent experiments were carried out with a metal loading of 1 wt% Pd. These results were confirmed by the corresponding turnover frequencies (TOF, Fig. 5(b)). The highest TOF was obtained with 1 wt% Pd. At lower Pd loadings, less active centers were present, while in the opposite direction, no improvement was seen with an excess of catalytic centers. A similar relationship was shown with the TOF for the conversion of **1** plotted against reaction
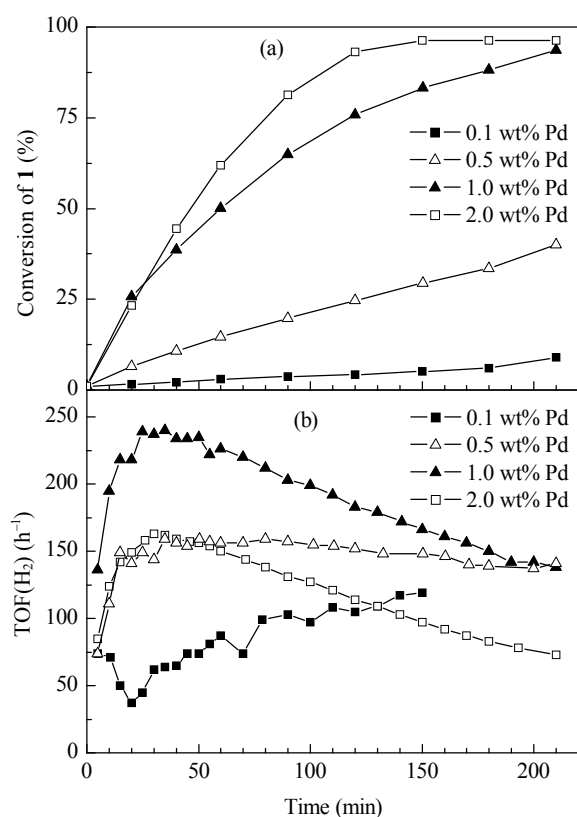
Table 5 Rate constants and time for 25%, 50%, and 75% conversion of **1** using various solvents

Solvent	k_1^a/(ml$_{H_2}$/min)	k_2^a/min^{-1}	Time for conversion of **1** (min)		
			25%	50%	75%
Chloroform	1.076	0.0046	210	—	—
Dioxane	2.017	*	65	210	—
Acetone	2.092	0.0043	40	90	150
Ethyl acetate	3.014	0.0023	20	60	120
2-Propanol	3.113	0.0042	20	70	150
Methanol	3.945	0.0028	25	60	120
Ethanol	4.236	0.0032	15	50	105

Reaction conditions: substrate **1** 15 mmol, catalyst 0.4 g Pd/TB (0.24 mol% Pd, Pd loading 1 wt% Pd), solvent 60 ml, T = 25 °C, p(H$_2$) = ambient pressure. ^{a}The rate constants k_1 and k_2 were estimated with linear regression. Following acceptances are made: liquid-phase hydrogenation is a reaction of pseudo zero-order and become a reaction of pseudo first-order at the end of reaction time. ^{b}Over the complete chosen time range the curve progression is linear with the same slope (pseudo-zero order reaction).

time. In the course of the reduction of **1,** the TOF decreased in all cases and reached 150 h^{-1}.

When the liquid phase hydrogenation of **1** was performed in different solvents, interesting effects were observed. The solvents and rate constants (k_1 and k_2) for hydrogenation with Pd/TB at room temperature and atmospheric pressure are summarized in Table 5. The chemoselective hydrogenation of the C-C double bond in **1** with the Pd catalyst was not affected by the solvent. **1a** was the only product. The polarity and hydrophilicity of the solvents increased from chloroform to ethanol (Table 5). These effects influenced the reaction rate and led to an increase of the rate constant k_1 with increasing solvent polarity. This was attributed to the fact that a polar media has good hydrogen absorption capacity. Thus, the gas-liquid diffusion barrier for the mass transport of molecular hydrogen to the active centers of the catalyst was lower. The decrease in the mass transport limitation of the solvents was shown by an increase of k_1. Complete conversion of **1** was detected after 210 min for acetone, ethyl acetate, 2-propanol, methanol, and ethanol. The three alcohols showed the highest initial hydrogenation rates, but all polar solvents showed complete conversion within the chosen time range. The solvents dioxane and chloroform (both non-polar) showed less hydrogen absorption capacity. This had a direct influence on the reaction rate for the reduction of **1**. Only 50% (dioxane) and 25% (chloroform) conversion of **1** were obtained after a reaction time of 210 min. This effect was manifested in the smaller rate constants k_1 with these solvents. The purity of the solvent played an important role in the liquid phase hydrogenation. No reduction of **1** was detected using solvents with a purity < 98%. The small amounts of impurities inhibited the hydrogen absorption capacity or/and contaminated the catalyst. The rate constant k_2
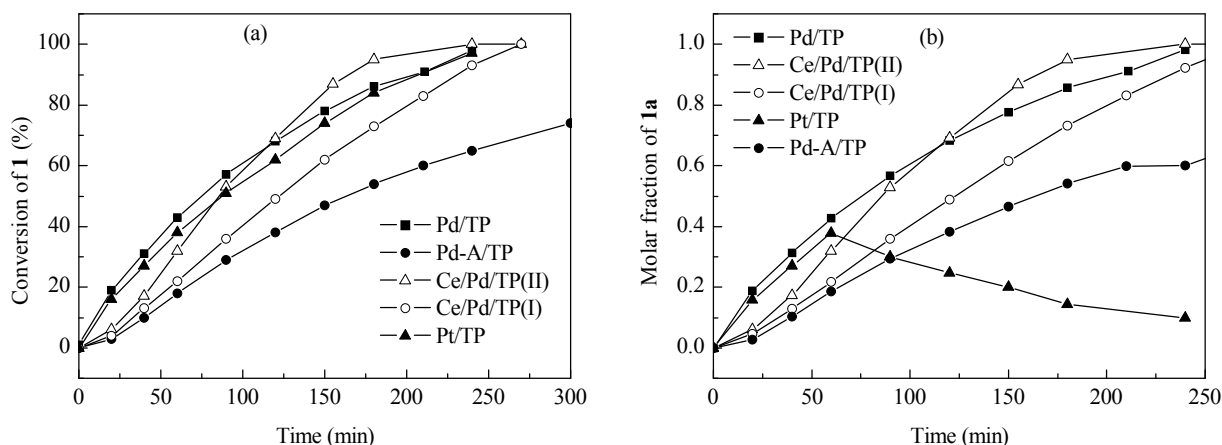

Fig. 5. Conversion of **1** (a) and hydrogen uptake TOF (b) using catalyst Pd/TB with different metal loadings at room temperature and atmospheric pressure. Reaction conditions are the same as in Table 4.

Fig. 6. Time dependence of the conversion of **1** and molar fraction of **1a** using various metals on porous glass at room temperature and atmospheric pressure. Reaction conditions: 15 mmol **1**, 0.24 mol% metal/TP, metal loading = 0.09 mmol/g, 60 ml ethyl acetate.

was in the same range for all the solvents and indicated the change from the diffusion controlled regime to reaction control. This is accompanied by a change of reaction order from pseudo-zero to pseudo-first order. In the range of k_2 the substrate **1** was the limiting reactant and not the reaction gas hydrogen like before (range of k_1).

Finally, the choice of solvent had an important influence on the reaction rate and conversion of the reactant. The solvent must have good hydrogen absorption capacity to get optimal results for the hydrogenation. All following experiments were carried out with ethyl acetate because of its polar character and hydrophilic properties.

Figure 6(a) illustrates the catalyst systems with different metal components and their activities in the liquid phase hydrogenation of **1** under the conditions used (25 °C, atmospheric pressure). All the catalysts except for Pd-A/TP gave complete conversion within 210 min. The reason for the low activity of Pd-A/TP was the metal precursor PdCl₂ employed for the preparation of this catalyst. The calcination temperature of the catalyst (450 °C) was below the decomposition temperature of PdCl₂ (675 °C; see Table 2). Therefore, traces of chloride remained on the surface and contaminated the active centers of the catalyst. Thus, in situ reduction of the Pd(II)-species to the catalytic active Pd(0) was suppressed, which was shown in the oxidation state of Pd deduced from the XPS data (Table 3). This led to the observed decrease in catalytic activity. A similar behavior was observed for the change of the oxidation state for RhCl₃ (Rh/TP; Table 3). All the catalysts reduced chemoselectively the conjugated C-C double bond at room temperature and atmospheric pressure. The only exception was Pt/TP. Figure 6(b) shows the molar fraction of the product **1a**. In the case of Pt/TP, a decrease of molar fraction after 50 min was detected, indicating the occurrence of a consecutive reaction pathway. The analysis showed the reduction of the C-O double bond and the formation of the product 1,3-diphenylpropan-1-ol (**1b**; Scheme 1). No influence of Ce on the hydrogenation of **1**

was observed when the experimental results were compared with those of the Ce-free Pd-catalyst Pd/TP. These results are in agreement with the observations from the XPS data described above regarding the change in oxidation state of Ce and Pd in the bimetallic catalysts (Table 3). Neither dehydration nor reduction of the aromatic double bond was found. The catalysts Rh/TP, Rh-A/TP, Ru/TP, Ru-A/TP, Au/TP, Ag/TP, Ir/TP, Co/TP, and Fe/TP showed no catalytic activity under the conditions employed.

2.3 Liquid phase hydrogenation under moderate temperature (≤ 50 °C) and pressure (≤ 0.8 MPa)

Reduction reactions under moderate conditions ($T \leq 50$ °C, $p \leq 0.8$ MPa) were carried out in the microwave reactor QRS described in the experimental section. The porous glass support used was TP impregnated with different metals (Table 2). All the catalysts that showed catalytic activity under the selected conditions are displayed in Table 6. The influence of reaction temperature on the hydrogenation of **1** with Pd/TP as catalyst at 0.4 MPa is shown in Fig. 7. The reduction was also chemoselective since only **1a** was found in the product. Reaction at room temperature (25 °C) gave a maximum conversion of

Table 6 Conversion of **1** due to the catalyst and reaction temperature

Catalyst	Conversion of **1** (%)	
	25 °C	50 °C
Pd/TP	73	99
Pd-A/TP	14	18
Ce/Pd/TP(I)	92	99
Ce/Pd/TP(II)	65	99
Pt/TP	58	99
Rh/TP	40	99
Rh-A/TP	17	99

Reaction conditions: 7.5 mmol **1**, 30 ml ethyl acetate, 0.24 mol% M/TP, metal loading = 0.09 mmol/g, p_{H2} = 0.8 MPa, reaction time 40 min, MultiSynth 400 W, ramp time 2 min.
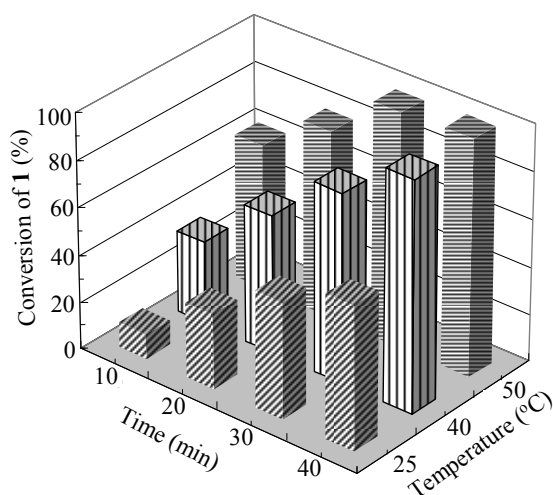
Fig. 7. Conversion of **1** at different temperatures. Reaction conditions: 7.5 mmol **1**, 30 ml ethyl acetate, 0.2 g Pd/TP (0.24 mol% Pd), $p_{H2} = 0.4$ MPa, continuous mode, reaction time 40 min, MultiSynth 400 W, ramp time 2 min.

Fig. 8. Conversion of **1** with various catalysts at different conditions. (1) $t = 30$ min, $p_{H2} = 3.0$ MPa; (2) $t = 30$ min, $p_{H2} = 5.0$ MPa; (3) $t = 90$ min, $p_{H2} = 3.0$ MPa; (4) $t = 90$ min, $p_{H2} = 5.0$ MPa. Other conditions: 7.5 mmol **1**, 30 ml ethyl acetate, 0.24 mol% M/TP, metal loading = 0.09 mmol/g, 25 °C.

65%. The higher temperature and pressure gave complete conversion within 30 or 40 min reaction time at 50 or 40 °C reaction temperature, respectively. Similar results were found for the reaction at elevated hydrogen pressure (0.6 MPa) since only the conversions at low temperature and short reaction time were slightly enhanced. Thus, the experiments proved that the experimental set-up was suitable for performing hydrogenation reactions under microwave irradiation with gaseous hydrogen as the reducing agent [6,19,34–39]. The change from conventional to microwave-assisted heating did not affect the course of reaction. Increased conversions at a shorter time (Fig. 6) were rather attributed to the elevated hydrogen pressure and/or reaction temperature and not to the microwave. No cooperative effect in both methods was seen from the spectroscopic analysis of the catalyst and the reaction data.

The catalytic activities with various metal catalysts at two different reaction temperatures (25 and 50 °C) are compared in Table 6. The catalysts and metal precursors employed are described in Table 2. The reduction was carried out at 0.8 MPa hydrogen pressure to use the maximum possible pressure in the QRS microwave system. Therefore, moderate pressure and temperature conditions were used, which can be compared with the results described earlier. All the catalysts except Pd-A/TP gave complete conversion of **1** at 0.8 MPa and 50 °C. At room temperature (25 °C) only Pd/TP and Ce/Pd/TP(I) gave acceptable conversions. The influence of temperature was especially large for the Rh-containing systems (Rh/TP and Rh-A/TP). The catalysts Pd/TP, Pd-A/TP, Ce/Pd/TP(I), and Ce/Pd/TP(II) chemoselectively reduced the C-C double bond and only product **1a** was identified. The Rh- and Pt-containing systems showed the reduction of the C-O double bond too. During the reaction time (40 min) 2%–4% of **1b** were formed (Scheme 1), in agreement with published results [40]. Under
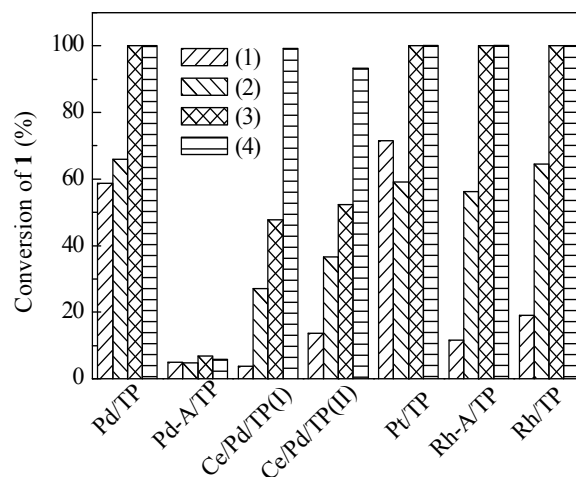
the reaction conditions used, a reduction of the aromatic C-C double bonds was not observed. All the catalysts not listed in Table 6 showed no catalytic activity (Table 2). These metals are well known to have catalytic activity only under extreme conditions (often gas phase reduction) or in homogenous catalysis [41–43].

2.4 Liquid phase hydrogenation under higher pressures (≤ 5.0 MPa) and room temperature

After reaction under moderate conditions, an increase of pressure was studied by performing the model reaction in stainless steel autoclaves. Figure 8 summarizes the results of the reduction of **1** with different catalysts. The experiments were undertaken with an upper pressure limit of 5.0 MPa at room temperature. All the catalysts except Pd-A/TP showed complete conversion at 5.0 MPa and 90 min. A reaction time of 30 min was not sufficient in all cases. The best results (conversion of **1** > 50%) were achieved with Pd/TP, Pt/TP, Rh/TP, and Rh-A/TP. The use of Ce-containing catalysts (Ce/Pd/TP(I) and Ce/Pd/TP(II)) and the use of Pd/TP and Pd-A/TP gave product **1a** only. The reduction of the C-C double bond was chemoselective in these cases. The addition of Ce to the catalyst had no influence on the selectivity, but led to a decreased conversion, probably due to blocking of the active Pd centers. The smaller conversion of Pd-A/TP compared to Pd/TP was again attributed to residual chloride on the surface due to an insufficient calcination temperature. Consecutive reactions of **1a** were found in the case of Pt/TP, Rh/TP and Rh-A/TP.

In particular, with the catalyst Pt/TP, different further reduction products were detected (Table 7). Subsequent to the formation of **1a,** the carbonyl group in **1a** was reduced giving **1b** when the hydrogen pressure was increased from 1.0 to 3.0

Table 7 Distribution of products for the hydrogenation of **1** and the dependence on the hydrogen pressure

Reactant and corresponding products	Molar fraction at different p_{H2}		
	1.0 MPa	3.0 MPa	5.0 MPa
1	0.16	0	0
1a	0.41	0.29	0.33
1b	0.43	0.62	0.61
1c	0	0.07	0.03
1e	0	0.01	0.02
1f	0	0.01	0.01

Reaction conditions: 7.5 mmol **1**, 30 ml ethyl acetate, 0.2 g Pt/TP (0.24 mol%), 25 °C, reaction time 90 min.

MPa. Simultaneously, dehydration of **1b** to 1,3-diphenylpropene (**1d**) as intermediate on hydrogenation increase to 1,3-diphenylpropane (**1e**). Furthermore, the addition of hydrogen to the phenyl rings was detected yielding 3-cyclohexyl-1-phenylpropan-1-one (**1c**) and 3-cyclohexyl-1-phenylpropane (**1f**). In addition, the catalysts Rh/TP and Rh-A/TP also gave small amounts of these products (Σ < 3%). Due to the fast reduction of the C–C double bond in **1d**, neither this intermediate product nor the completely saturated product 1,3-dicyclohexylpropane (**1g**) was detected. The performance of liquid phase hydrogenation at 5.0 MPa and room temperature revealed that the catalysts Ir/TP, Au/TP, Ru/TP, Fe/TP, and Ru-A/TP were not active under the applied experimental conditions.

3 Conclusions

Porous glass can be applied as a support material in heterogeneous catalysis, especially in the liquid phase hydrogenation of benzalacetophenone. It can be impregnated with various metal precursors to give a wide variety of metal catalysts. Reactions under higher pressure and temperature can be carried out without any change in support parameters like surface area and porosity. With an increase in pressure from atmospheric to 5.0 MPa, shorter reaction times are possible. Some catalysts (Rh/TP and Rh-A/TP) showed catalytic activity only at higher pressures. The influences of the solvent, metal precursor, and metal loading with catalyst Pd/TB were investigated under mild reaction conditions (room temperature, atmospheric pressure).

Acknowledgments

References

1 Swift K A D. *Top Catal*, 2004, **27**: 143

2 Monteiro J L F, Veloso C O. *Top Catal*, 2004, **27**: 169

3 Pérez-Cadenas A F, Kapteijn F, Ziverink M M P, Moulijn J A. *Catal Today*, 2007, **128**: 13

4 Tonetto G M, Sánchez J F, Ferreira M L, Damiani D D. *J Mol Catal A*, 2009, **299**: 88

5 Schmidt A, Schomäcker R. *J Mol Catal A*, 2007, **271**: 192

6 Schmöger C, Stolle A, Bonrath W, Ondruschka B. *Curr Org Chem*, 2011, **15**: 151

7 Mennecke K, Cecilia R, Glasnov T N, Gruhl S, Vogt C, Feldhoff A, Vargas M A L, Kappe C O, Kunz U, Kirschning A. *Adv Synth Catal*, 2008, **350**: 717

8 Sharma A, Kumar V, Sinha A K. *Adv Synth Catal*, 2006, **348**: 354

9 Pillai U R, Sahle-Demessi E, Varma R S. *J Mater Chem*, 2002, **12**: 3199

10 Vanier G S. *Synlett*, 2007: 131

11 Chtourou M, Abdelhedi R, Krikha M H, Trabelsi M. *Ultrason Sonochem*, 2010, **17**: 246

12 Wang H S, Zeng J. *Can J Chem*, 2009, **9**: 1209

13 Balini R, Bosica G, Ricciutelli M, Maggi R, Sartori G, Sartorio R, Righi P. *Green Chem*, 2001, **3**: 178

14 Cho C S, Ren W X, Yoon N S. *J Mol Catal A*, 2009, **299**: 117

15 Trost B M, Xu J Y, Schmidt T. *J Am Chem Soc*, 2009, **131**: 18343

16 Schmöger C, Stolle A, Bonrath W, Ondruschka B, Keller T, Jandt K D. *ChemSusChem*, 2009, **2**: 77

17 Bonrath W, Ondruschka B, Schmöger C, Stolle A. WO 2010/020671 A1. 2010

18 Schmöger C, Gallert T, Stolle A, Ondruschka B, Bonrath W. *Chem Eng Technol*, 2011, **34**: 445

19 Schmöger C, Szuppa T, Tied A, Schneider F, Stolle A, Ondruschka B. *ChemSusChem*, 2008, **1**: 339

20 Li J T, Mau A W H, Strauss C R. *Chem Commun*, 1997: 1275

21 Enke D, Janowski F, Schwieger W. *Microporous Mesoporous Mater*, 2003, **60**: 19

22 Gille W, Enke D, Janowski F. *J Phys Chem Solids*, 2003, **64**: 2

23 Weyrich P A, Trevin H, Hoelderich W F, Sachtler W M H. *Appl Catal A*, 1997, **163**: 31

24 Feuerriegel U, Klose W. *Chem Ing Tech*, 1998, **70**: 449

25 Yazawa Y, Yoshida H, Takagi N, Komai S I, Satsuma A, Hattori T. *Appl Catal B*, 1998, **19**: 261

26 Huang L, Wang Z, Ang T P, Tan J, Wong P K. *Catal Lett*, 2006, **112**: 219

27 Reddy J K, Durgakumari V, Subrahmanyam M, Sreedhar B. *Mater Res Bull*, 2009, **44**: 1540

28 Korsvik C, Patil S, Seal S, Self W T. *Chem Commun*, 2007: 1056

29 Matsumura Y, Kagawa K, Usami Y, Kawazoe M, Sakurai H, Haruta M. *Chem Commun*, 1997: 657

30 Contreras A M, Yan X-M, Kwon S, Bokor J, Somorjai G A. *Catal Lett*, 2006, **111**: 5

31 Del C Aguirre M, Reyes R, Oportus M, Melian-Cabrera I, Fierro J L G. *Appl Catal A*, 2002, **233**: 183

32 Vanier G. WO 2007/103501 A2. 2007

33 Gustafsson T, Hedenstrom M, Kihlberg J. *J Org Chem*, 2006, **71**: 1911

34 Heller E, Lautenschläger W, Holzgrabe U. *Tetrahedron Lett*, 2005, **46**: 1247

35 Piras L, Genesio E, Ghiron C, Taddei M. *Synlett*, 2008: 1125

36 Ma Y M, Wei X Y, Zhou X, Cai K Y, Peng Y L, Xie R L, Zong Y, Wei Y B, Zong Z M. *Energ Fuels*, 2009, **23**: 638

37 Hsieh Y C, Chir J L, Zou W, Wu H H, Wu A T. *Carbohydrate Res*, 2009, **344**: 1020

38 Reyes P, Rojas H, Pecchi G, Fierro J. *J Mol Catal A*, 2002, **179**: 293

39 Ning J B, Xu J, Liu J, Lu F. *Catal Lett*, 2006, **109**: 175

40 Moura F C C, dos Santos E N, Lago R M, Vargas M D, Araujo M H. *J Mol Catal A*, 2005, **226**: 243

41 Chou J, Franklin N R, Baeck S-H, Jaramillo T F, McFarland E W. *Catal Lett*, 2004, **95**: 107